

Fluorine-Free Hydrophobic Polymer Brushes for Self-Healing Coatings

Annemieke van Dam, Sidharam P. Pujari, Maarten M. J. Smulders,* and Han Zuilhof*

Cite This: *ACS Appl. Nano Mater.* 2024, 7, 19737–19744

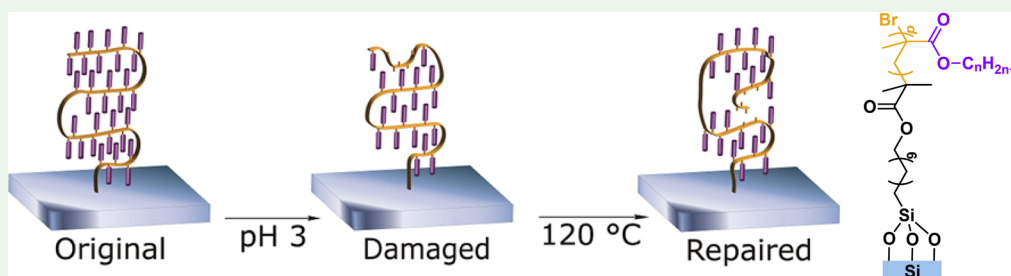
Read Online

ACCESS |

Metrics & More

Article Recommendations

Supporting Information



ABSTRACT: Fluorinated hydrocarbons are excellent building blocks for hydrophobic coatings but also yield undesirable toxicity and environmental persistence. In precision industries such as high-resolution printing, polymer brushes are a valuable tool, as they can be tuned on the nanometer scale and can impart the underlying surface with desired properties and/or functionalities. Here, we report that the beneficial properties typically associated with (partially) fluorinated polymer brush coatings can to a large degree also be achieved with their nonfluorinated counterparts. To this end, we have successfully grafted 13 poly(alkyl methacrylate) homopolymer brushes from a flat silicon surface using surface-initiated atom transfer radical polymerization (SI-ATRP). These polymer brushes were characterized by XPS, ellipsometry, and static water contact angle measurements. They were then shown to be repeatedly self-repairing by thermal treatment at 120 °C after damage by pH 3, with longer side chains being more resistant to damage from the acid. Branching of the side chains did not significantly influence this resistance, but it lowered the static water contact angle. Some polymer brushes with intermediate side chain length displayed an increase in the contact angle over the first four cycles. This was not caused by impurities but was the result of an annealing effect that improved the packing of the side chains of the brushes. In all, these coatings are suitable, self-healing, environmentally friendly, and fully nonfluorinated alternatives for current fluorine-based hydrophobic coatings.

KEYWORDS: hydrophobic coating, polymer brush, self-healing, fluorine-free, surface-initiated atom transfer radical polymerization

INTRODUCTION

Hydrophobic surfaces are essential for a smooth operation in, for example, oil processing,^{1,2} heat exchangers,³ inkjet printing, and polymer production.⁴ The butterfly wing⁵ but also the upper part of a lotus leaf⁶ are well-known, highly attractive natural hydrophobic surfaces: chemically unreactive with water and both nano- and macrostructured. Most synthetic hydrophobic coatings have taken one or more aspects of the lotus leaf as inspiration. That is, 3D structures have been created to reduce the contact area with a water droplet, thus increasing the contact angle, leading to superhydrophobicity.^{7–10} In such cases, the structural integrity of the coating is crucial, and damage leads to significant loss of functionality.^{11–13} Furthermore, without the use of a chemical coating, this structural repellence works only for solvents with a high surface tension.

Well-known examples of such coatings are those in which long polyfluorinated aliphatic chains are used. Examples like polytetrafluoroethylene (PTFE/Teflon)^{14–16} and perfluorinated silanes^{17–20} are often applied as nonreactive coatings

on industrial scales but also for medical purposes and kitchen utensils.²¹ However, increasing knowledge on their toxicity and carcinogenicity^{22–24} in combination with their environmental persistence displays serious drawbacks, and the use of per- and polyfluoroalkyl substances (PFAS) should be drastically reduced.²⁵ In line with this, more and more countries are restricting or forbidding the use of PFAS.²⁶ In contrast to their environmental persistence, the lifetime of such coatings is typically limited, as they lend their antifouling ability to low surface tension which is easily disturbed.

As recently reviewed,²⁷ many highly elegant approaches have been designed to obtain coatings that are able to withstand

Received: July 12, 2024

Revised: July 18, 2024

Accepted: July 22, 2024

Published: August 6, 2024



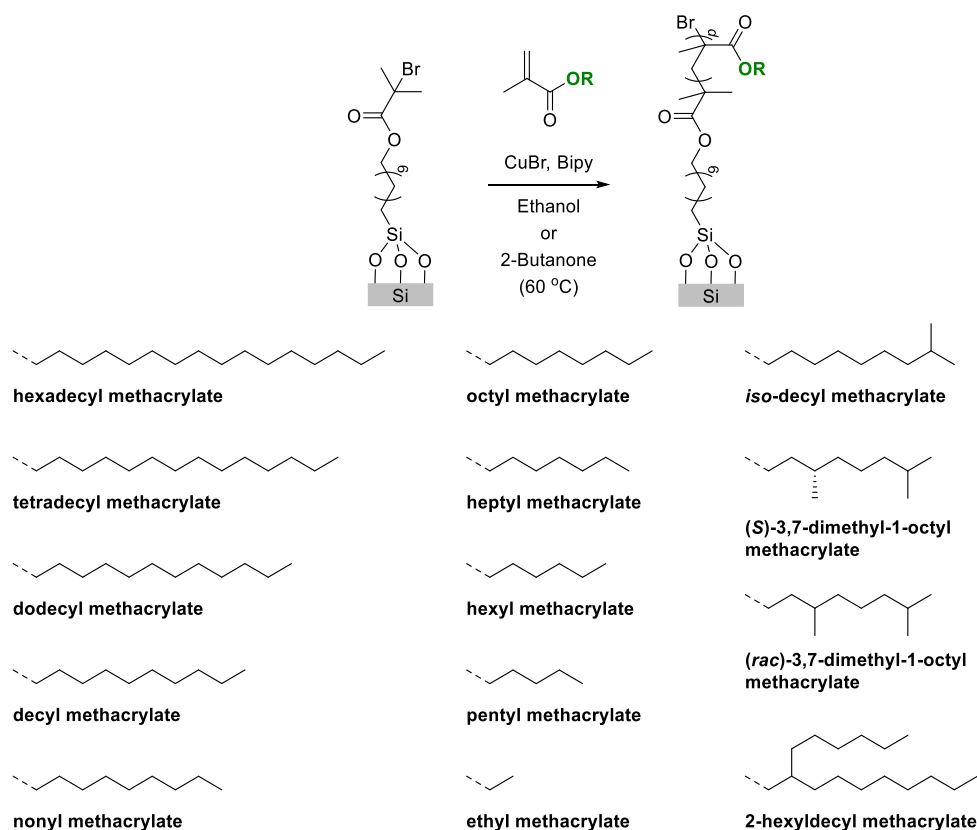


Figure 1. Schematic depiction of the self-repairing polymer brushes with side chains accentuated in green (top) and the general synthesis and structure of the studied polymer brushes (bottom).

damage by the incorporation of a self-repair mechanism.^{27–32} However, although the possibility of self-repair after damage may significantly extend the device lifetime, the removed part is still lost to the environment. As all of the aforementioned examples are carbon–fluorine-based, release of these fluorine-containing parts has a persistent, negative environmental impact. Finding nonfluorinated hydrophobic coatings is thus urgently needed. The group of Hozumi developed an oil-repellent polymer brush through A(R)GET-ATRP from (dimethylamino)ethyl methacrylate, thus using an environmentally friendly method to create a fluorine-free coating.³³ As polymer brushes are covalently attached to the surface, a strong, lasting connection is formed.³⁴ By grafting them from the surface, the thickness can be closely controlled and precise knowledge of the chemical composition is maintained. Nanoscale alterations can be performed, if required, for the intended application. Due to this precision, polymer brushes have been developed as coatings for various applications, ranging from antibiofouling^{35,36} via thermoresponsiveness^{37,38} to lubrication^{39,40} and nanosensors.⁴¹ In previous research,³² we have produced such a self-repairing polymer brush-based coating as well. In that report, next to a study of a series of fluorinated polymer brushes, we provided preliminary evidence that poly(decyl methacrylate) (which is fluorine-free, hydrophobic, and polymer repelling) is resistant to damage by pH 3. In contrast, their fluorinated counterparts were damaged by the same solution. Additionally, poly(pentyl methacrylate) and poly(ethyl methacrylate) were not resistant to the pH 3 solution either but were repairable by placement in the oven at 120 °C. Although we were positively surprised by this result, we did not have a full explanation at that time.

Intrigued by these initial findings and in light of the need for robust, fluorine-free hydrophobic coatings, in this paper, the effect of the alkyl side chain of a poly(alkyl methacrylate) brush on both the stability (in pH 3) and capacity for self-repair is investigated. A range of linear side chains is investigated, from ethyl to hexadecyl (Figure 1). As micelle research by Brady^{42–44} has shown that alkyl chains can form impenetrable sheets from eight carbons and longer, we expected a change in stability behavior beyond a certain alkyl chain length. In addition, since branching of the alkyl chains may affect such sheet formation, it is highly relevant to also study the effects thereof on the coating stability and self-repair capabilities.

This paper outlines the synthesis of some hitherto not reported alkyl methacrylate monomers, including four with branched alkyl moieties, the polymer brush formation of 14 of these monomers by surface-initiated atom transfer radical polymerization (SI-ATRP), the characterization of the resulting coating by ellipsometry, X-ray photoelectron spectroscopy (XPS), and static water contact angle measurements, and studies of the polymer brush structure after damage by acid (pH 3) and annealing. Finally, it provides a comparative analysis of fluorinated and nonfluorinated polymer-brush coatings and outlines the significant potential of the latter in view of the reported observations.

RESULTS AND DISCUSSION

Setup of Study and Monomers Involved. The effect of the side chain structure on the self-healing capability of 14 polymer brushes was investigated with a range of homopolymer brushes (Figure 1). First, we studied 10 methacrylates

Table 1. Polymer Brush Formation of the Methacrylates under Study: Reaction Conditions, Average Coating Thickness, and Static Water Contact Angle (WCA)^a

monomer	solvent	polymerization time (h)	coating thickness (nm)	WCA (deg)
Hexadecyl methacrylate	2-Butanone ^b	24	23 ± 11	107 ± 1
Tetradecyl methacrylate	2-Butanone ^c	24	113 ± 5	107 ± 1
Dodecyl methacrylate	2-Butanone	40	125 ± 8	105 ± 3
Decyl methacrylate	2-Butanone	26	114 ± 5	102 ± 3
Nonyl methacrylate	2-Butanone	48	40 ± 3	96 ± 3
	Ethanol ^c	24	139 ± 12	
Octyl methacrylate	Ethanol ^c	20	69 ± 11	94 ± 3
Heptyl methacrylate	Ethanol ^c	24	87 ± 28	90 ± 4
Hexyl methacrylate	Ethanol	20	111 ± 38	87 ± 2
Pentyl methacrylate	2-Butanone	48	66 ± 3	86 ± 1
	Ethanol ^c	46	64 ± 5	
Ethyl methacrylate	Ethanol	8	85 ± 6	76 ± 1
Isodecyl methacrylate	Ethanol	8	103 ± 26	94 ± 2
(<i>S</i>)-3,7-Dimethyl-1-octyl methacrylate	Ethanol	48	143 ± 7	96 ± 1
(<i>rac</i>)-3,7-Dimethyl-1-octyl methacrylate	Ethanol	24	65 ± 12	95 ± 1
2-Hexyldecyl methacrylate	2-Butanone	48	61 ± 44	105 ± 3

^aReactions were performed at 60 °C with 1 mol % CuBr catalyst, 2 mol % bpy ligand, 25 vol% monomer, and 75 vol% solvent. Thickness variation within a surface was about 5 nm. Indicated thickness deviations are between different surfaces of the same batch. ^bWith 4,4'-dinonyl-bipyridine (dnbpy) as ligand instead of 2,2'-bipyridine (bpy). ^cDouble catalyst and ligand concentration.

with linear side chains consisting of 2–16 carbons. Then, to also investigate the effect of branching, we studied decyl methacrylate and two of its isomers, isodecyl methacrylate and 3,7-dimethyl-1-octyl methacrylate, the latter in both enantiopure and racemic forms. Additionally, we studied 2-hexyldecyl methacrylate, an isomer of hexadecyl methacrylate with 10 carbons in its longest chain and therefore displaying two branches of considerable length.

Eight of the monomers studied were commercially available. The other six (heptyl-, octyl-, nonyl-, (*S*)-3,7-dimethyl-1-octyl-, (*rac*)-3,7-dimethyl-1-octyl-, and (*rac*)-2-hexyldecyl methacrylate) were synthesized on gram scale, via the acid-catalyzed esterification of methacrylic acid, with isolated yields between 75% and 89% (see Supporting Information sections S4–S9, respectively, for details on the synthesis and characterization).

Polymer Brush Formation. A previously reported³² SI-ATRP protocol was performed on initiator-activated silicon surfaces to obtain homopolymer brushes of all 14 methacrylates (Supporting Information section S3). A batch of silicon surfaces was activated by sonication and oxygen plasma cleaning before being submerged in a solution of 3-(trichlorosilyl)propyl-2-bromo-2-methylpropanoate in toluene at room temperature for 16 h. Subsequently, the polymerization reaction was performed by placing 10 of thus coated silicon surfaces in a reactor in a nitrogen atmosphere glovebox in a polymerization solution (8–48 h at 60 °C; see for further details Table 1 and Supporting Information Figure S1). The preparation of the polymerization solution was done in the glovebox as well. After polymerization, the surfaces were placed in a vacuum oven at 50 °C and 50 mbar overnight for further drying. The surfaces were then analyzed by ellipsometry, static water contact angle measurements, and XPS (see for details Supporting Information section S10), with the characteristic results given in Table 1. For three types of surfaces, the advancing and receding contact angles were determined as well, both in horizontal state and at a 30° tilt (Supporting Information section S12, Table S2). Sliding angles were not found: the water remained on the surfaces, even at 180° tilt.

Polymer brush formation was performed until coatings of at least 60 nm thickness were obtained, as we required the brush regime of the tethered polymer chains. We expected similar polymerization rates for all side chain lengths; however, we found a large variation in coating thickness after 24 h (data not shown). We therefore optimized the reaction conditions for each monomer to reach at least 60 nm thickness (Table 1). In some instances, double catalyst and ligand concentrations were used in order to speed up the reaction. The longer methacrylates (C₁₀ and higher) did not mix well with ethanol, which we thus substituted with 2-butanone. Decyl-, dodecyl-, and tetradecyl methacrylate polymerized well in this solvent. While these varying polymerization conditions resulted in difference polymerization rates between different monomers/surfaces, from earlier work³² (based on AFM) we could infer that our polymerization method (for a given monomer/surface) does yield smooth surfaces (with a roughness in the order of 1–3 nm).

The exception was hexadecyl methacrylate, for which the use of either ethanol or 2-butanone as solvent did not provide coatings of more than 40 nm, even after reacting for 96 h (Supporting Information section S11, Table S1). An average of 23 nm was obtained in 2-butanone after 24 h. Toluene, 1-pentanol, 1-octanol, or 1-decanol as solvent, both at 60 °C and at 100 °C and using 4,4'-dinonyl-bipyridine as alternative ligand, did not work well either for this monomer: no more than 15 nm of brush could be grown. Self-healing results of the thickest poly(hexadecyl methacrylate) brushes (Figure S18) showed vastly different behavior from that of poly(tetradecyl methacrylate), indicating poor surface coverage. This is most likely caused by poor polymerization due to low solubility of the monomer. Poly(hexadecyl methacrylate) should therefore not be included in the series for further experiments. In contrast, polymerization of its branched isomer 2-hexyl-1-decyl methacrylate was possible under the regular reaction conditions and only slightly longer reaction time. However, a large sample-to-sample variation in thicknesses was observed, indicating that solute–solvent mixing was not ideal for 2-hexyl-1-decyl methacrylate either.

A clear linear correlation was visible between side chain length and the static water contact angle (Figure 2). The

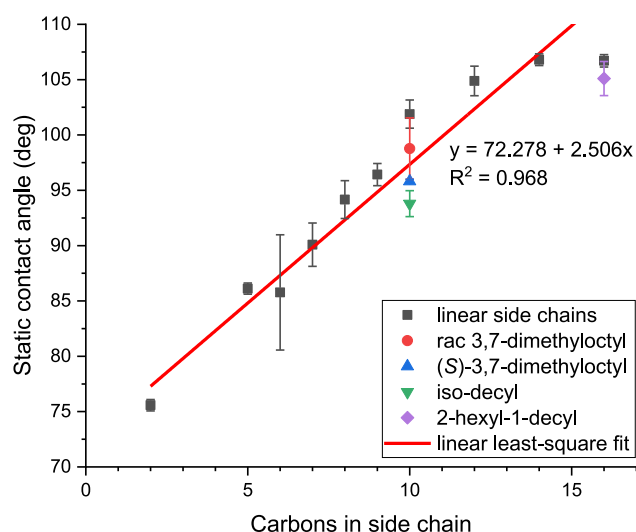


Figure 2. Correlation between the number of carbon atoms in the side chain of the polymer brush and the static water contact angle of this brush (from Table 1). A least-squares line is fitted through the contact angles of the coatings with linear side chains (black points only) and is described by a linear function.

relatively low static contact angle for the C_{16} brush could be explained by its low thickness, which would make the overall surface somewhat less hydrophobic (as compared to the trendline). For the other brushes, every carbon added to the length of the side chain added 2.7° to the contact angle, on average. The common threshold for hydrophobicity, 90° , was reached by seven carbon atoms in the alkyl side chains. The branched alkyl moieties did not behave according to their number of carbons but rather to their longest chain. For example, both racemic and enantiopure poly(3,7-dimethyloctyl methacrylate) had a static water contact angle of 95° , similar to the value of 94° for poly(octyl methacrylate). This indicated that the cross-section area of the polymer chains, determined by the length of the longest linear side chain, rather than number of carbon atoms per side chain dominated the hydrophobicity of the polymer brushes.

Polymer Brush Self-Repair. The self-repairing ability of the polymer brushes was tested by repeated placement in a pH 3 solution (HCl, for 24 h) and a 120°C oven (for 2 h), as done in previous research.³² After each step, the surfaces were blown dry, and their static water contact angles were measured (Figure 3). For poly(pentyl, nonyl, and dodecyl methacrylate), the advancing and receding contact angles were measured at each stage as well, at a 30° tilt (Supporting Information section S12). The polymers with shorter linear side chains (C_2 until C_7) displayed a clear zigzag pattern. Upon placement in acid, the contact angles decreased. This was most likely caused by acid-catalyzed hydrolysis of the ester bonds in the polymer, which removed the aliphatic chain and left only carboxylic acid on the backbone of the polymer. As the carboxylic acid is more hydrophilic than the aliphatic chain, the water contact angle decreased. As this affected the receding contact angle more than the advancing, an increase in hysteresis was observed for poly(pentyl methacrylate) in Figure S19. Upon placement in the oven, full recovery of the original contact angles was observed, indicating that the hydrophobic top layer was

restored. We hypothesize that upon heating above the glass transition temperature, the polymer brush rearranges itself in the thermodynamically most favorable way. The acidic groups will cluster together, while the hydrophobic side chains will be pushed outward (Scheme 1). A near-pristine top layer reforms, displaying the same hydrophobicity as before the damage took place. As the glass transition temperatures of poly(*n*-alkyl methacrylates) are shown to be lower with each additional carbon,⁴⁵ starting with 74°C for poly(ethyl methacrylate),⁴⁶ we can assume that at 120°C , all the studied polymer brushes are well above their glass transition temperature.

While the polymer brushes with short side chains showed a clear zigzag pattern, the damage of polymer brushes with longer side chains was much less pronounced. In the poly(octyl methacrylate) brush some damage and repair could be observed, but poly(nonyl, decyl, dodecyl, and tetradecyl methacrylate) brushes even looked mostly unaffected by the acid. The hysteresis between advancing and receding contact angle for poly(nonyl methacrylate) remained constant as well and even reversed for a few cycles in poly(dodecyl methacrylate) (Figures S20 and S21, respectively). We hypothesize that the long linear alkyl chains stack to form a closely packed sheet that is impenetrable by acid. As the acid cannot reach the ester moieties, no hydrolysis takes place, and thus no damage to the coating occurs. Already in the 1970s such close packing of alkyl chains was mentioned in micelle formation, with a turning point around eight carbons.⁴³

We have now observed a similar turning point for the stability of methacrylate-based polymer brushes with alkyl side chains: clear damage of, e.g., poly(heptyl methacrylate) brushes, slight damage of poly(octyl methacrylate) brushes, and no significant damage of the brushes composed of poly(nonyl methacrylate) and longer, linear poly(alkyl methacrylates). IRRAS analysis confirmed this sheet formation, as the signal for C–H stretching was shifted from 2932 cm^{-1} in poly(pentyl methacrylate) to 2925 and 2926 cm^{-1} in poly(dodecyl methacrylate) and poly(nonyl methacrylate), respectively (Supporting Information section S13).⁴⁷ Additionally, AFM studies (see Supporting Information, section S15) confirmed that a polymer brush with a short side chain (C_5) could be damaged in acidic (pH 3) conditions, as evidenced from the increased surface roughness). The damaged, roughened surface could subsequently be healed by thermal treatment (as evidenced by a reduction in surface roughness). In contrast, the longer chain (C_{12}) coating was unaffected by the acidic conditions and did not undergo a healing step during the thermal treatment, as was observed by the largely unchanged surface roughness.

The low stability of the poorly grafted poly(hexadecyl methacrylate) (Supporting Information section S11) was another indicator that sheet formation prevented damage. Although the side chains were of sufficient length to prevent hydrolysis, the coating was so poorly grafted that no full sheet of alkyl chains was formed, offering no protection against acid hydrolysis. As a result, large changes in contact angle were observed after each damage (around 100°) and repair (around 107°) half-cycle.

We hypothesized that branching of the side chains could disrupt the sheet formation of the side chains, thereby allowing hydrolysis to take place in branched polymer brushes with side chains above eight carbons. Poly(isodecyl methacrylate) displayed some damage and repair after cycle four, indicating that its packing is not as tight as in poly(decyl methacrylate).

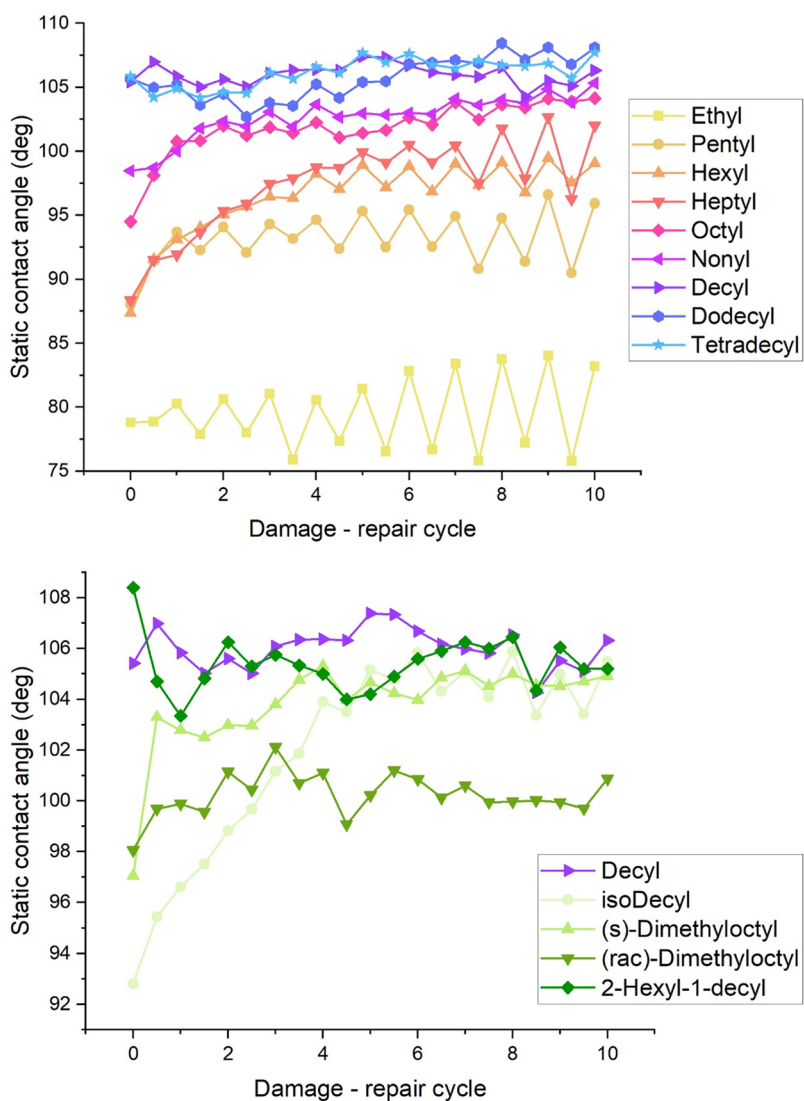
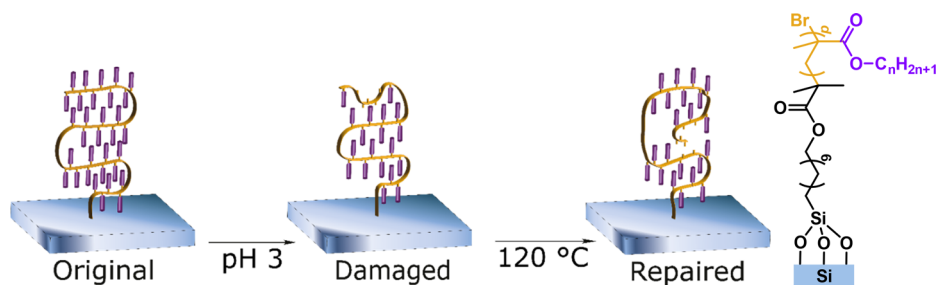


Figure 3. Self-repair of the linear polymer brushes (top) and the branched polymer brushes (bottom). The static water contact angle was measured after each damaging step (half-cycle points) and after each healing step (whole cycle points). The error margins are around 1° for all points and are omitted for clarity.

Scheme 1. Proposed Self-Repair Mechanism^{32,a}



^aIn an acidic environment, some of the ester bonds will be broken and the side chains will be removed. Upon heating, rearrangements occur: the acid groups will cluster together in the bulk of the polymer, and a full top layer returns. A color-coded schematic representation of the polymer is provided on the right.

However, both types of poly(3,7-dimethyloctyl methacrylate) showed no damage. Apparently, the disruption caused by the methyl on the end of the side chain could be mitigated by the methyl closer to the ester bond, providing additional

hydrophobic shielding to the nearby ester group. This occurred regardless of the enantiopurity of the side chain.

Disruption of the packing by a larger side chain did not have much of an effect either. Poly(2-hexyl-1-decyl methacrylate) showed the same contact angle and stability as poly(decyl

methacrylate). No effect of the branching hexyl group was observed. We thus note that although branches close to the ester bond could disrupt the packing of alkyl chains, they remain effective in protecting the ester from acidic hydrolysis, likely by a combination of increased local hydrophobicity and steric hindrance. In contrast, branching at the end of the side chains reduced the robustness of the polymer brush, which we hypothesize to be due to the reduction of the interdigitation of alkyl chains inside the brush: branching at the end of the alkyl chain would most affect this interdigitation.

The stability of the coatings was also tested at other pHs. Repeated submersion of poly(decyl methacrylate) in HCl solutions of pH 1 and 2 showed no damage (Supporting Information section S14), indicating complete stability in acid. Full stability in NaOH solutions of pH 11 and 13 was found as well. Upon submersion at pH 14, the entire polymer brush was removed from the surface, indicating breaking of the silane bond rather than the ester of the methacrylates.

Annealing Phase. In the first four damage–repair cycles, the static water contact angle of poly(hexyl methacrylate) steadily increased (Figure 3). Poly(heptyl methacrylate), poly(octyl methacrylate), and poly(isodecyl methacrylate) also displayed this behavior. We hypothesized that either contamination (that is released during the immersion in pH 3 solution) or poor packing of the side chains could disrupt the behavior of the polymer brushes at the start of the experiments, leading to a slightly reduced contact angle.

To establish whether the reduction of the contact angle was caused by contamination, we first tried to wash out any contamination by immersion. To this end, we placed some poly(hexyl methacrylate) surfaces in Milli-Q for 24 h, then in the oven for 2 h, and then again in Milli-Q and the oven. This mimicked the first two self-repair cycles but with pH 7 instead of pH 3, thus doing no damage. After this treatment, we performed 10 damage–repair cycles as usual (Figure 4, blue line). Although a slight increase in the contact angle in the first cycle could be seen, no significant improvement was found. Contamination that is gradually washed out is thus unlikely to cause disruption of the contact angle.

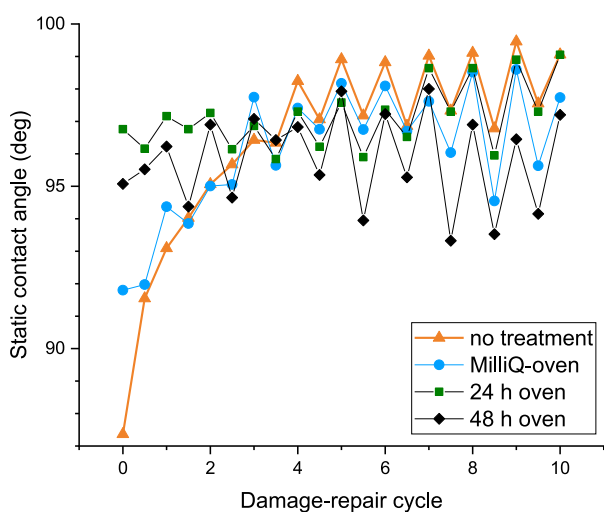


Figure 4. Self-repair cycles of poly(hexyl methacrylate) without any treatment (orange), after Milli-Q oven treatment (blue), after 24 h oven treatment (dark green), and after 48 h oven treatment (black).

If the disruption of the contact angle is caused by poor packing, then no damage or solvation steps are necessary to solve the problem, only annealing at an elevated temperature for a specific period of time above the glass transition temperature. To investigate this hypothesis, we placed new surfaces in an oven at 120 °C for 48 h and measured their contact angles (Table 2). Indeed, the starting contact angles of

Table 2. Static Water Contact Angles of Polymer Brushes before and after Curing for 48 h at 120 °C

monomer	WCA (deg) before	WCA (deg) after
Dodecyl methacrylate	105 ± 3	99
Decyl methacrylate	102 ± 3	99 ± 2
Nonyl methacrylate	96 ± 3	98 ± 2
Octyl methacrylate	94 ± 3	99 ± 2
Heptyl methacrylate	90 ± 4	99 ± 1
Hexyl methacrylate	87 ± 2	95 ± 2
Pentyl methacrylate	86 ± 1	89 ± 2
Ethyl methacrylate	76 ± 1	76 ± 1
Isodecyl methacrylate	94 ± 2	95 ± 3

most coatings were higher than without the pretreatment. This supports the hypothesis that the initial coatings do not yet have the most optimal packing, which is only obtained after high-temperature annealing. It also explains why the shorter, more flexible, chains suffer most from this phenomenon: the longer chains have more driving force for correct packing and thus will pack in the most stable configuration from the start.

Furthermore, poly(hexyl methacrylate) surfaces were placed in the oven for 24 h, after which the self-repair experiments were performed (Figure 4, dark green line). This proved to be long enough to allow relaxation into the ideal configuration, with no more annealing visible in the first few cycles and a stable, high contact angle throughout the 10 cycles. Lastly, self-repair experiments were performed with the poly(hexyl methacrylate) surfaces that were placed in an oven for 48 h (Figure 4, black line). Although these displayed consistent contact angles, the values were slightly lower than after only 24 h oven treatment or no pretreatment. As a result, 24 h appears to be the optimal pretreatment time.

CONCLUSIONS

Fourteen covalently linked nonfluorinated polymer brushes were produced and shown to be self-repairing upon heating after damage by pH 3 in 10 damage–repair cycles. Longer linear side chains not only displayed higher hydrophobicity but were also better able to withstand such damage. With short side chains ($\leq C_8$), an increase in hydrophobicity was observed over the first few cycles, indicating that the packing of chains was improved with every cycle. Longer chains did not show this: they were packed closely from the start.

The high hydrophobicity, durability, and self-healing capability of nonfluorinated polymer brushes are highly desirable, as replacements for fluorinated coatings are urgently needed. Simultaneously, the nanoscale precision of polymer brushes as hydrophobic coatings remains essential for heat exchangers, inkjet printing, and related industries. In an age where fluorinated compounds have fallen from their throne as ideal coatings, these nonfluorinated polymer brushes are shown to be worthy heirs.

■ ASSOCIATED CONTENT

SI Supporting Information

The Supporting Information is available free of charge at <https://pubs.acs.org/doi/10.1021/acsanm.4c03988>.

Materials, methods, synthesis, and characterization of monomers, production and characterization of polymer brushes, additional figures and tables, and additional references that include refs 48 and 49 (PDF)

■ AUTHOR INFORMATION

Corresponding Authors

Maarten M. J. Smulders – Laboratory of Organic Chemistry, Wageningen University and Research, 6708 WE Wageningen, The Netherlands; orcid.org/0000-0002-6855-0426; Email: maarten.smulders@wur.nl

Han Zuilhof – Laboratory of Organic Chemistry, Wageningen University and Research, 6708 WE Wageningen, The Netherlands; School of Pharmaceutical Sciences and Technology, Tianjin University, 300072 Tianjin, China; orcid.org/0000-0001-5773-8506; Email: han.zuilhof@wur.nl

Authors

Annemieke van Dam – Laboratory of Organic Chemistry, Wageningen University and Research, 6708 WE Wageningen, The Netherlands; orcid.org/0000-0003-1112-4597

Sidharam P. Pujari – Laboratory of Organic Chemistry, Wageningen University and Research, 6708 WE Wageningen, The Netherlands; orcid.org/0000-0003-0479-8884

Complete contact information is available at: <https://pubs.acs.org/doi/10.1021/acsanm.4c03988>

Author Contributions

The manuscript was written through contributions of all authors. All authors have given approval to the final version of the manuscript.

Notes

The authors declare no competing financial interest.

■ ACKNOWLEDGMENTS

This research was carried out under Project S62.3.15577 in the framework of the Partnership Program of the Materials Innovation Institute M2i (www.m2i.nl) and the Technology Foundation TTW, which is part of The Netherlands Organization for Scientific Research (www.nwo.nl).

■ REFERENCES

- (1) Bockstahler, T. E.; Hunt, C. R. Prevention of Polymer Fouling of Monomer Processing Apparatus. Patent US3705190, 1969.
- (2) Feng, L.; Zhang, Z.; Mai, Z.; Ma, Y.; Liu, B.; Jiang, L.; Zhu, D. A Super-Hydrophobic and Super-Oleophilic Coating Mesh Film for the Separation of Oil and Water. *Angew. Chem., Int. Ed.* **2004**, *43* (15), 2012–2014.
- (3) Kuschnerow, J. C.; Dorn, S.; Augustin, W.; Scholl, S. Investigations of Polymer Fouling on Heated and Cooled Surfaces. *Proceedings of International Conference on Heat Exchanger Fouling and Cleaning; Heat Exchanger Fouling and Cleaning*, 2013; pp 150–157.
- (4) McFadden, D. M.; Wu, R. S.-H. The Reduction of Polymer Fouling on Reactor Surfaces in a Continuous Process for Preparing Polymers. Patent US6380324B1, 2000.
- (5) Wagner, T.; Neinhuis, C.; Barthlott, W. Wettability and Contaminability of Insect Wings as a Function of Their Surface Sculptures. *Acta Zoologica* **1996**, *77* (3), 213–225.

- (6) Ensikat, H. J.; Ditsche-Kuru, P.; Neinhuis, C.; Barthlott, W. Superhydrophobicity in Perfection: The Outstanding Properties of the Lotus Leaf. *Beilstein J. Nanotechnol.* **2011**, *2*, 152–161.

- (7) Wang, D.; Sun, Q.; Hokkanen, M. J.; Zhang, C.; Lin, F. Y.; Liu, Q.; Zhu, S. P.; Zhou, T.; Chang, Q.; He, B.; Zhou, Q.; Chen, L.; Wang, Z.; Ras, R. H. A.; Deng, X. Design of Robust Superhydrophobic Surfaces. *Nature* **2020**, *582* (7810), 55–59.

- (8) Haghdoost, A.; Pitchumani, R. Fabricating Superhydrophobic Surfaces via a Two-Step Electrodeposition Technique. *Langmuir* **2014**, *30* (14), 4183–4191.

- (9) Shibuichi, S.; Onda, T.; Satoh, N.; Tsujii, K. Super Water-Repellent Surfaces Resulting from Fractal Structure. *J. Phys. Chem.* **1996**, *100*, 19512–19517.

- (10) Öner, D.; McCarthy, T. J. Ultrahydrophobic Surfaces. Effects of Topography Length Scales on Wettability. *Langmuir* **2000**, *16* (20), 7777–7782.

- (11) Yamamoto, M.; Nishikawa, N.; Mayama, H.; Nonomura, Y.; Yokojima, S.; Nakamura, S.; Uchida, K. Theoretical Explanation of the Lotus Effect: Superhydrophobic Property Changes by Removal of Nanostructures from the Surface of a Lotus Leaf. *Langmuir* **2015**, *31* (26), 7355–7363.

- (12) Tian, X.; Verho, T.; Ras, R. H. A. Moving Superhydrophobic Surfaces toward Real-World Applications. *Science* **2016**, *352* (6282), 142–143.

- (13) Verho, T.; Bower, C.; Andrew, P.; Franssila, S.; Ikkala, O.; Ras, R. H. A. Mechanically Durable Superhydrophobic Surfaces. *Adv. Mater.* **2011**, *23* (5), 673–678.

- (14) Sarkar, D. K.; Farzaneh, M.; Paynter, R. W. Superhydrophobic Properties of Ultrathin RF-Sputtered Teflon Films Coated Etched Aluminum Surfaces. *Mater. Lett.* **2008**, *62* (8–9), 1226–1229.

- (15) Nelson, E.; Kilduff, T. J.; Benderly, A. A. Bonding of Teflon. *Ind. Eng. Chem.* **1958**, *50* (3), 329–330.

- (16) Dhanumalayan, E.; Joshi, G. M. Performance Properties and Applications of Polytetrafluoroethylene (PTFE)—a Review. *Adv. Compos. Hybrid. Mater.* **2018**, *1* (2), 247–268.

- (17) Denes, A. R.; Tshabalala, M. A.; Rowell, R.; Denes, F.; Young, R. A. Hexamethyldisiloxane-Plasma Coating of Wood Surfaces for Creating Water Repellent Characteristics. *Holzforschung* **1999**, *53*, 318–326.

- (18) Akamatsu, Y.; Makita, K.; Inaba, H.; Minami, T. Water-Repellent Coating Films on Glass Prepared from Hydrolysis and Polycondensation Reactions of Fluoroalkyltrialkoxysilane. *Thin Solid Films* **2001**, *389*, 138–145.

- (19) Alessandrini, G.; Aglietto, M.; Castelvetro, V.; Ciardelli, F.; Peruzzi, R.; Toniolo, L. Comparative Evaluation of Fluorinated and Unfluorinated Acrylic Copolymers as Water-Repellent Coating Materials for Stone. *Appl. Polym. Sci.* **2000**, *76* (6), 962–977.

- (20) Ivanova, N. A.; Zaretskaya, A. K. Simple Treatment of Cotton Textile to Impart High Water Repellent Properties. *Appl. Surf. Sci.* **2010**, *257* (5), 1800–1803.

- (21) Pisani, E.; Tsapis, N.; Galaz, B.; Santin, M.; Berti, R.; Taulier, N.; Kurtisovski, E.; Lucidarme, O.; Ourevitch, M.; Doan, B. T.; Beloeil, J. C.; Gillet, B.; Urbach, W.; Bridal, S. L.; Fattal, E. Perfluoroethyl Bromide Polymeric Capsules as Dual Contrast Agents for Ultrasonography and Magnetic Resonance Imaging. *Adv. Funct. Mater.* **2008**, *18* (19), 2963–2971.

- (22) Fenton, S. E.; Ducatman, A.; Boobis, A.; DeWitt, J. C.; Lau, C.; Ng, C.; Smith, J. S.; Roberts, S. M. Per- and Polyfluoroalkyl Substance Toxicity and Human Health Review: Current State of Knowledge and Strategies for Informing Future Research. *Environ. Toxicol. Chem.* **2021**, *40* (3), 606–630.

- (23) Hekster, F. M.; Laane, R. W. P. M.; de Voogt, P. Environmental and Toxicity Effects of Perfluoroalkylated Substances. In *Reviews of Environmental Contamination and Toxicology*; Springer, 2003; Volume 179, pp 99–121, DOI: [10.1007/0-387-21731-2_4](https://doi.org/10.1007/0-387-21731-2_4).

- (24) Cao, Y.; Ng, C. Absorption, Distribution, and Toxicity of per- and Polyfluoroalkyl Substances (PFAS) in the Brain: A Review. *Environ. Sci. Processes Impacts* **2021**, *23* (11), 1623–1640.

- (25) Cousins, I. T.; Johansson, J. H.; Salter, M. E.; Sha, B.; Scheringer, M. Outside the Safe Operating Space of a New Planetary Boundary for Per- and Polyfluoroalkyl Substances (PFAS). *Environ. Sci. Technol.* **2022**, *56* (16), 11172–11179.
- (26) <https://echa.europa.eu/-/echa-publishes-pfas-restriction-proposal> (accessed April 23, 2023).
- (27) Wang, Z.; Zuilhof, H. Self-healing superhydrophobic fluoropolymer brushes as highly protein-repellent coatings. *Langmuir* **2016**, *32* (25), 6310–6318.
- (28) Li, Y.; Li, L.; Sun, J. Bioinspired Self-Healing Superhydrophobic Coatings. *Angew. Chem., Int. Ed.* **2010**, *49* (35), 6129–6133.
- (29) Wang, X.; Liu, X.; Zhou, F.; Liu, W. Self-Healing Superamphiphobicity. *Chem. Commun.* **2011**, *47* (8), 2324–2326.
- (30) Esteves, A. C. C.; Luo, Y.; Van De Put, M. W. P.; Carcouët, C. C. M.; De With, G. Self-Replenishing Dual Structured Superhydrophobic Coatings Prepared by Drop-Casting of an All-in-One Dispersion. *Adv. Funct. Mater.* **2014**, *24* (7), 986–992.
- (31) Garcia, S. J. Effect of Polymer Architecture on the Intrinsic Self-Healing Character of Polymers. *Eur. Polym. J.* **2014**, *53*, 118–125.
- (32) van Dam, A.; Smulders, M. M. J.; Zuilhof, H. Self-Healing Antifouling Polymer Brushes: Effects of Degree of Fluorination. *Appl. Surf. Sci.* **2022**, *579*, No. 152264.
- (33) Dunderdale, G. J.; Urata, C.; Miranda, D. F.; Hozumi, A. Large-Scale and Environmentally Friendly Synthesis of pH-Responsive Oil-Repellent Polymer Brush Surfaces under Ambient Conditions. *ACS Appl. Mater. Interfaces* **2014**, *6* (15), 11864–11868.
- (34) Zoppe, J. O.; Ataman, N. C.; Mocny, P.; Wang, J.; Moraes, J.; Klok, H. A. Surface-Initiated Controlled Radical Polymerization: State-of-the-Art, Opportunities, and Challenges in Surface and Interface Engineering with Polymer Brushes. *Chem. Rev.* **2017**, *117* (3), 1105–1318.
- (35) Kuzmyn, A. R.; Nguyen, A. T.; Teunissen, L. W.; Zuilhof, H.; Baggerman, J. Antifouling Polymer Brushes via Oxygen-Tolerant Surface-Initiated PET-RAFT. *Langmuir* **2020**, *36* (16), 4439–4446.
- (36) Glinel, K.; Jonas, A. M.; Jouenne, T.; Leprince, J.; Galas, L.; Huck, W. T. S. Antibacterial and Antifouling Polymer Brushes Incorporating Antimicrobial Peptide. *Bioconjugate Chem.* **2009**, *20* (1), 71–77.
- (37) Teunissen, L. W.; Kuzmyn, A. R.; Ruggeri, F. S.; Smulders, M. M. J.; Zuilhof, H. Thermoresponsive, Pyrrolidone-Based Antifouling Polymer Brushes. *Adv. Mater. Interfaces* **2022**, *9* (6), No. 2101717.
- (38) Jones, D. M.; Smith, J. R.; Huck, W. T. S.; Alexander, C. Variable Adhesion of Micropatterned Thermoresponsive Polymer Brushes: AFM Investigations of Poly(*N*-Isopropylacrylamide) Brushes Prepared by Surface-Initiated Polymerizations. *Adv. Mater.* **2002**, *14* (16), 1130–1134.
- (39) Kreer, T. Polymer-Brush Lubrication: A Review of Recent Theoretical Advances. *Soft Matter* **2016**, *12* (15), 3479–3501.
- (40) Sakakibara, K.; Maeda, K.; Yoshikawa, C.; Tsujii, Y. Water Lubricating and Biocompatible Films of Bacterial Cellulose Nanofibers Surface-Modified with Densely Grafted, Concentrated Polymer Brushes. *ACS Appl. Nano Mater.* **2021**, *4* (2), 1503–1511.
- (41) Zhu, H.; Masson, J.-F.; Bazuin, G. Templating Gold Nanoparticles on Nanofibers Coated with a Block Copolymer Brush for Nanosensor Applications. *ACS Appl. Nano Mater.* **2020**, *3* (1), 516–529.
- (42) Brady, G. W. Effect of Length on the Interaction of Dissolved Long Chain Molecules. *J. Chem. Phys.* **1973**, *58* (9), 3542–3546.
- (43) Brady, G. W. On the Aggregation of Dissolved Alkane Chain Molecules. *Acc. Chem. Res.* **1974**, *7* (6), 174–180.
- (44) Brady, G. W. On the Aggregation of Mixtures of Long and Short Chain Molecules. *J. Chem. Phys.* **1974**, *60* (9), 3466.
- (45) Beiner, M.; Schröter, K.; Hempel, E.; Reissig, S.; Donth, E. Multiple Glass Transition and Nanophase Separation in Poly(*n*-Alkyl Methacrylate) Homopolymers. *Macromolecules* **1999**, *32* (19), 6278–6282.
- (46) Garwe, F.; Schonhals, A.; Lockwenz, H.; Beiner, M.; Schroter, K.; Donth, E. Influence of Cooperative a Dynamics on Local b Relaxation during the Development of the Dynamic Glass Transition in Poly(*n*-Alkyl Methacrylate)s. *Macromolecules* **1996**, *29* (1), 247–253.
- (47) Snyder, R. G.; Strauss, H. L.; Elliger, C. A. Carbon-hydrogen stretching modes and the structure of *n*-alkyl chains. 1. Long, disordered chains. *J. Phys. Chem.* **1982**, *86* (26), 5145–5150.
- (48) Pierce, E.; Carmona, F. J.; Amirfazli, A. Understanding of sliding and contact angle results in tilted plate experiments. *Colloids Surf., A* **2008**, *323*, 73–82.
- (49) Montes Ruiz-Cabello, F. J.; Rodríguez-Valverde, M. A.; Cabrerizo-Vílchez, M. A new method for evaluating the most stable contact angle using tilting plate experiments. *Soft Matter* **2011**, *7*, 10457–10461.